RSC Advances

REVIEW

View Article Online
View Journal | View Issue

Cite this: *RSC Adv.*, 2017, **7**, 43410

Magnetic, magnetocaloric and critical behavior investigation of $La_{0.7}Ca_{0.1}Pb_{0.2}Mn_{1-x-y}Al_xSn_yO_3$ (x, y = 0.0, 0.05 and 0.075) prepared by a sol–gel method

Khadija Dhahri, *[a] N. Dhahri,[a] J. Dhahri, [a] K. Taibi,[b] E. K. Hlil,[c] Hafedh Belmabrouk[d] and M. Zaidi[d]

A systematic study on the magnetic, magnetocaloric and critical behavior properties of polycrystalline $La_{0.7}Ca_{0.1}Pb_{0.2}Mn_{1-x-y}Al_xSn_yO_3$ prepared *via* a sol–gel method are studied. These compounds present a single magnetic transition from a ferromagnetic (FM) to paramagnetic (PM) phase with decreasing temperature. The critical exponents are estimated using various techniques, such as a modified Arrott plot, the Kouvel–Fisher method and critical isotherm analysis based on the data of static magnetic measurements recorded around the Curie temperature, T_C. The estimated critical exponent values are found to be consistent and comparable to those predicted by the 3D-Ising model for x, y = 0.0 and by the mean field model for x, y = 0.05 and 0.075. We have confirmed the obtained critical exponents with the single scaling equation: $M(\mu_0 H,\varepsilon) = \varepsilon^{\beta} f \pm (\mu_0 H/\varepsilon^{\beta+\gamma})$, where $\varepsilon = (T - T_C)/T_C$ is the reduced temperature. We have investigated the validity and usefulness of theoretical modeling in our compound $La_{0.7}Ca_{0.1}Pb_{0.2}Mn_{1-x-y}Al_xSn_yO_3$ based on the mean-field analysis of the magnetic entropy change ($-\Delta S_M$) *versus* the magnetization data. For comparison, the M_{Sp} has been also deduced from the classical extrapolation of the Arrott plot. We obtain an excellent agreement between the spontaneous magnetization determined from the entropy change ($-\Delta S_M$ *vs.* M^2) and the Arrot curves ($\mu_0 H/M$ *vs.* M^2), confirming the validity of the magnetic entropy change approach in order to estimate the spontaneous magnetization M_{Sp} in a ferromagnetic system.

Received 6th April 2017
Accepted 24th July 2017

DOI: 10.1039/c7ra03913a

rsc.li/rsc-advances

1. Introduction

In the last few decades, magnetic refrigeration in the room-temperature range has attracted global interest owing to its energy-efficient and environment-friendly advantages over the gas compression–expansion refrigeration techniques.[1,2] It is based on the magnetocaloric effect (MCE), which is the thermal response (heating or cooling) of a magnetic substance when a magnetic field is applied or removed. Recently, much research in this area has been to develop materials that are cost effective and exhibit large MCE (large isothermal magnetic entropy change ΔS_M) over a wide temperature range. Among them, lanthanum manganites with the general formula $La_{1-x}A_xMnO_3$, where A is a divalent element (A = Ca, Sr, Ba…), have drawn the attention of the solid-state physics community because of their important electrical and magnetic properties, such as the discovery of their colossal magnetoresistance (CMR)[3–7] and the magnetocaloric effect (MCE).[8–13] These materials exhibit a rich variety of physical properties. The most accepted interpretations for the cause of these properties are the double exchange model[14] and Jahn–Teller effect.[15,16] Both of these mechanisms are used to identify the magnetic phase transition (FM–PM).[17] To understand better the metal–semiconductor transition and the CMR, it is important to fully understand the nature of the PM–FM transition. Therefore, to make these issues clear, it will be essential to cross over on the critical exponents at the region of the paramagnetic (PM)–ferromagnetic (FM) transition in order to unveil the nature of the magnetic system transition. Up to date, a great number of reports on the critical behaviors around the Curie temperature have been predicted that the critical exponents play important roles in elucidating interactions mechanisms near T_C. Most attention has been focused on the study of the critical phenomena of La-based manganites.[18–30] On the one side, in an earlier theoretical work, the critical behavior in the DE model was first described with long range mean-field theory.[31] On the other side, some researchers have reported that the critical exponents in manganites are in

[a]*Laboratoire de la matière condensée et des nanosciences, Département de Physique, Faculté des Sciences, Université de Monastir, Monastir 5019, Tunisia. E-mail: khadijadhahri91@yahoo.com*

[b]*Département SDM, FGMGP/USTHB, 16311, Algeria*

[c]*Institut Néel, CNRS-Université J. Fourier, BP 166, Gronoble 38042, France*

[d]*Department of Physics, College of Science of Zulfi, Majmaah University, Al Majmaah, Saudi Arabia*

agreement with a short-range exchange-interaction model[32] with the estimated critical exponent values related to either 3D-Heisenberg[33] or 3D-Ising[34] model. Several studies[35–38] have been carried out on the vicinity of the magnetic phase transition by using a variety of techniques have yielded a wide range of values for the critical parameters β. For example the β value reported by Ghosh *et al.*[39] is equal to 0.37 for the ferromagnet manganite $La_{0.7}Sr_{0.3}MnO_3$. However, Amaral *et al.*[40] reported that the values of the critical exponents for $La_{0.665}Eu_{0.035}Sr_{0.3}MnO_3$ are in good agreement with that predicted by the mean-field theory. Meanwhile, in the series of compounds $La_{1-x}Ca_xMnO_3$, there exists a tricritical point at $x = 0.4$ that sets a boundary between first-order ($x < 0.4$) and second-order ($x > 0.4$) FM phase transition in the FM range ($0.2 < x < 0.5$).[41] Up to now, in view of the various critical exponents β from 0.1 to 0.5, four kinds of different theoretical models, which are mean-field theory($\beta = 0.5$, $\gamma = 1.0$ and $\delta = 3.0$), 3D-Ising model ($\beta = 0.325$, $\gamma = 1.241$ and $\delta = 4.82$) 3D-Heisenberg model ($\beta = 0.365$, $\gamma = 1.336$ and $\delta = 4.8$) and tricritical mean field theory ($\beta = 0.25$, $\gamma = 1.0$ and $\delta = 5.0$), were used to discuss the critical properties in manganites.

In the present work, a detailed investigation is conducted on magnetic, magnetocaloric properties and the critical behaviors in the polycrystalline $La_{0.7}Ca_{0.1}Pb_{0.2}Mn_{1-x-y}Al_xSn_yO_3$ (x, y = 0.0, 0.05 and 0.075) by using various techniques through modified Arrot plot, Widom scaling and Kouvel–Fisher methods. We demonstrate that the critical phenomena near PM–FM Curie temperature transition is described by mean-field model and 3D-Ising model rather than by the two others models. Consequently, from the magnetic entropy change determined from magnetic measurements ($-\Delta S_M$ *vs.* M^2), we have estimated the spontaneous magnetization (M_{Sp}) and the results of this approach are compared with the classical extrapolation of the Arrott curves (μ_0H/M *vs.* M^2).

2. Experimental details

$La_{0.7}Ca_{0.1}Pb_{0.2}Mn_{1-x-y}Al_xSn_yO_3$ (x, y = 0.0, 0.05 and 0.075) compounds were prepared using a conventional sol–gel method that details was described in our previous work.[42] The magnetization measurements were carried out using a vibrating sample magnetometer developed in Louis Néel Laboratory at Grenoble, where we measured the magnetization *versus* applied magnetic field in a temperature range near T_C. To extract the critical exponent of the samples accurately, isothermal magnetization data as function of magnetic field were performed in the range of 0–5 T, in the vicinity of the PM to FM phase transition. These isothermals are corrected by a demagnetization factor D that has been determined by a standard procedure from low-field dc magnetization measurement at low temperatures ($\mu_0H = \mu_0H_{app} - DM$).

3. Scaling analysis

The scaling hypothesis suggests the following power-law relation near the critical region defined by:

$$M_S(T) = M_0(-\varepsilon)^{\beta},\ \varepsilon < 0 \quad (1)$$

$$\chi_0^{-1}(T) = (h_0/M_0)\varepsilon^{\gamma},\ \varepsilon > 0 \quad (2)$$

$$M = DH^{1/\delta},\ \varepsilon = 0 \quad (3)$$

where ε is the reduced temperature $\varepsilon = (T - T_C)/T_C$ and M_0, h_0 and D are the critical amplitudes. Moreover, according to the prediction of the scaling equation in the asymptotic critical region, the magnetic equation of state can be written as:

$$M(\mu_0H,\varepsilon) = \varepsilon^{\beta}f \pm (\mu_0H/\varepsilon^{\beta+\gamma}) \quad (4)$$

where f_+ and f_- are regular analytical functions above and below T_C (ref. 43 and 44). This last eqn (4) indicates that for true scaling relations and right choice of β, γ and δ values, the scaled $M/|\varepsilon|^{\beta}$ plotted as a function of the scaled $\mu_0H/|\varepsilon|^{\beta+\gamma}$ will fall on two universal curves, one for temperatures $T > T_C$ ($\varepsilon > 0$) and the other for $T < T_C$ ($\varepsilon < 0$). This is an important criterion of critical regime.

4. Results and discussion

4.1. Magnetic and magnetocaloric properties

The magnetization of $La_{0.7}Ca_{0.1}Pb_{0.2}Mn_{1-x-y}Al_xSn_yO_3$ (x, y = 0.0, 0.05, and 0.075) as a function of temperature in a 0.05 T magnetic field in both zero-field-cooled (ZFC) and field-cooled (FC) processes of all the samples has been undertaken and their behavior is shown in Fig. 1. Based on these results, it appears that with decreasing temperature, the samples exhibit a magnetic transition from a paramagnetic (PM) to a ferromagnetic (FM) state, at the same time, T_C slightly decreases with small (Al, Sn) concentration, then this transition shifts towards room temperature on adding more (Al, Sn) content. Consequently, the Curie temperature for each sample, obtained from the inflection points of the derivative dM/dT, was found to be

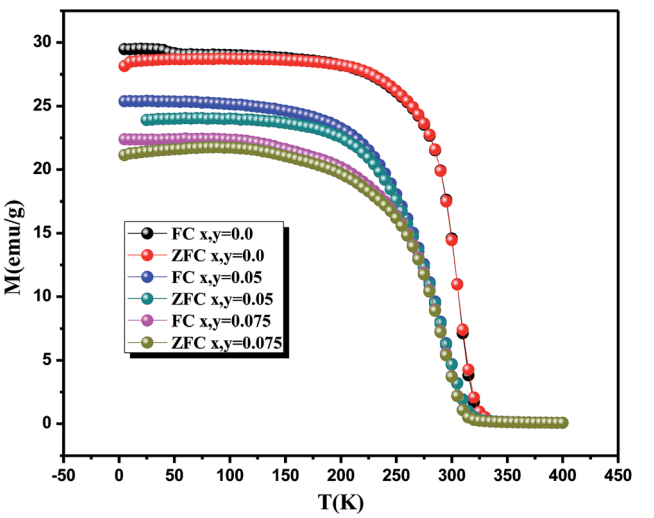

Fig. 1 Temperature dependences of ZFC and FC magnetization for $La_{0.7}Ca_{0.1}Pb_{0.2}Mn_{1-x-y}Al_xSn_yO_3$ (x, y = 0.0, 0.05 and 0.075) compounds under a magnetic field of 0.05 T.

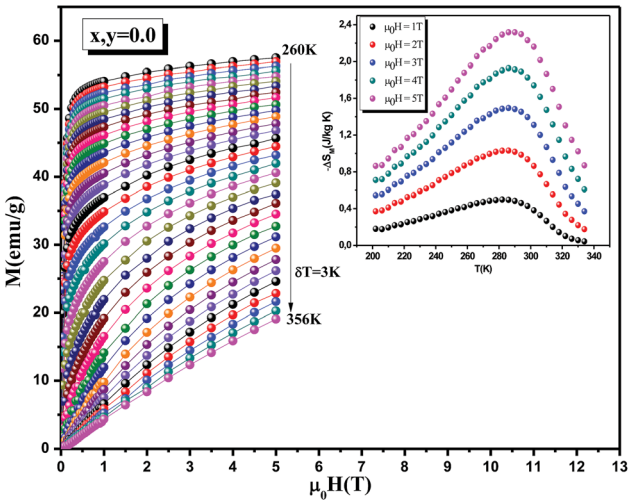

Fig. 2 Magnetic field dependence of magnetization at several temperatures for $La_{0.7}Ca_{0.1}Pb_{0.2}Mn_{1-x-y}Al_xSn_yO_3$ (x, y = 0.0) sample, the inset: temperature dependence of the magnetic entropy change ($-\Delta S_M$) at different applied magnetic field change intervals for $La_{0.7}Ca_{0.1}Pb_{0.2}Mn_{1-x-y}Al_xSn_yO_3$ (x, y = 0.05).

310 K, 295 K and 290 K for x, y = 0.0, 0.05 and 0.075, respectively. These values deduced are very close to room temperature, which are quite suitable for magnetic refrigeration technology. Obviously, below the Curie temperature one may distinguish the pronounced split between the field-cooled (FC) and zero-field-cooled (ZFC) for all samples. This prominent divergence has been attributed to the magnetic frustration arising from a coexistence of insulating antiferromagnetic and metallic ferromagnetic phases, or from the competition between antiferromagnetic and ferromagnetic interactions. The gradual decrease of T_C as well as the saturation magnetization (M_S) with increase of (Al, Sn) content indicates weakening of the double exchange ferromagnetic interactions associated with the itinerancy. The T_C reduction in $La_{0.7}Ca_{0.1}Pb_{0.2}Mn_{1-x-y}Al_xSn_yO_3$ samples with increasing (Al, Sn)-doping is in good agreement with the results reported by.[45,46]

Together with the $M(T)$ investigations, we have measured magnetic-field dependences of the initial magnetization, $M(\mu_0H)$, of the samples $La_{0.7}Ca_{0.1}Pb_{0.2}Mn_{1-x-y}Al_xSn_yO_3$ around their FM–PM phase transition. In Fig. 2, the isothermal magnetization *versus* applied field, with temperature increments of 3 K, is shown for $La_{0.7}Ca_{0.1}Pb_{0.2}MnO_3$ under magnetic field μ_0H ranging between 0 and 5 T. Below T_C, the magnetization saturates rapidly due to an easy orientation of the spins under the action of the applied field, which confirms the ferromagnetic behavior of our compounds at low temperatures. On the other site, for $T > T_C$ and above $\mu_0H = 1$ T, the mean value of the moment orientation is modified and an induced magnetization parallel to the field appears. This magnetization is all the smaller as the temperature is high, which means that the thermal agitation is important. Gradually as the temperature increases the variations of the magnetization as a function of the field become more and more linear reflecting a paramagnetic behavior.[47]

In order to enquire the efficiency of our sample in the magnetic refrigeration systems, the magnetic entropy change due to the application of a magnetic field H can be calculated from a family of isothermal M–μ_0H curves, using a numerical approximation as follows:

$$\Delta S_M(T, \mu_0H) = S_M(T, \mu_0H) - S_M(T, 0) = \int_0^{\mu_0H} \left(\frac{dM}{dT}\right)_H d\mu_0H \quad (5)$$

The magnetic entropy change between 0 and μ_0H magnetic applied field, can be basically obtained by:

$$\Delta S_M\left(\frac{T_1+T_2}{2}\right) = \frac{1}{T_2-T_1}\left[\int_0^{\mu_0H} M(T_2, \mu_0H)d\mu_0H - \int_0^{\mu_0H} M(T_1, \mu_0H)d\mu_0H\right] \quad (6)$$

The temperature dependence of the magnetic entropy change ($-\Delta S_M$) taken at various magnetic fields ranging from 1 to 5 T for x, y = 0.05 sample is shown in the inset of Fig. 2. One can see that, at a given temperature, the overall value of entropy change is found to increase with increasing field, and exhibited a maximum value around T_C. The magnetic entropy change ($-\Delta S_M$) reaches a maximum values of 3.7 J kg^{-1} K^{-1}, 2.3 J kg^{-1} K^{-1} and 2 J kg^{-1} K^{-1} obtained at corresponding temperatures 310 K, 295 K and 290 K for x, y = 0.0, 0.05 and 0.075, respectively, under a magnetic field of 5 T. From the application point view, the relative cooling power (RCP) can be, in simple cases, evaluated by considering the magnitude of $|\Delta S_M^{max}|$ and its full width at half maximum (δT_{FWHM}). We can see that these results are interesting compared with other compounds reported in the literature, so we can estimate that our materials are a potential candidate to be used in an ideal Ericsson refrigeration cycle. To further investigate the reliability of these values, we gathered in Table 1 the values of $-\Delta S_M^{max}$ and RCP for all the samples under a magnetic applied field of 5 T as well as some results found in previous works[48,55] in order to compare them with ours.

In order to understand the origin of the magnetocaloric effect described by the spin fluctuations, Amaral *et al.*[56,57] have proposed a successful model based on Landau's theory of phase transition, with a contribution from magnetoelastic and electron interaction in manganites. Using the Landau power expansion of the magnetization M, by neglecting higher-order parts, the Gibbs free energy *versus* magnetization and temperature can be expressed in the following form:

$$G(M, T) = G_0 + \frac{A(T)}{2}M^2 + \frac{B(T)}{4}M^4 + \frac{C(T)}{6}M^6 + \ldots - M\mu_0H \quad (7)$$

where $A(T)$ and $B(T)$ are called Landau coefficients, these coefficients depend on the temperature and containing the elastic and magnetoelastic free energy. From the condition of equilibrium; *i.e.* energy minimization $\left(\frac{\partial G}{\partial M}\right) = 0$, the magnetic equation of state is obtained as:

Table 1 Maximum entropy change $|\Delta S_M^{max}|$ and relative cooling power (RCP), for $La_{0.7}Ca_{0.1}Pb_{0.2}Mn_{1-x-y}Al_xSn_yO_3$ (x, y = 0.0, 0.05 and 0.075), occurring at the Curie temperature (T_C) and under magnetic field variations, ΔH = 1 T, 3 T or ΔH = 5 T, compared to several materials considered for magnetic refrigeration

Sample	T_C (K)	ΔH (T)	$-\Delta S_M^{max}$ (J kg^{-1} K^{-1})	RCP (J kg^{-1})	References
Gd	293	5	9.5	410	48
$Gd_5Si_2Ge_2$	275	5	18.5	535	49
$La_{0.67}Ba_{0.33}MnO_3$	292	5	1.48	161	50
$La_{0.7}Sr_{0.3}Mn_{0.9}Al_{0.1}O_3$	310	5	2.6	109	51
$La_{0.67}Ca_{0.33}MnO_3$	252	5	2.06	175	52
$La_{2/3}(Ca,Pb)_{1/3}MnO_3$	290	7	7.5	375	53
$La_{0.65}Ca_{0.35}Ti_{0.4}Mn_{0.6}O_3$	42	3	0.6	55	54
$La_{0.7}Pb_{0.3}MnO_3$	358	1.35	1.53	53	55
$La_{0.7}Ca_{0.1}Pb_{0.2}MnO_3$	310	5	3.7	145	This work
$La_{0.7}Ca_{0.1}Pb_{0.2}Mn_{0.9}Al_{0.05}Sn_{0.05}O_3$	295	5	2.3	135	This work
$La_{0.7}Ca_{0.1}Pb_{0.2}Mn_{0.85}Al_{0.075}Sn_{0.075}O_3$	290	5	2	176	This work

$$\mu_0 H/M = A(T) + B(T)M^2 + C(T)M^4 \quad (8)$$

In addition, the applied magnetic field $\mu_0 H$ can be deduced from eqn (8) as:

$$\mu_0 H = A(T)M + B(T)M^3 + C(T)M^5 \quad (9)$$

According to this equation, the values of $A(T)$, $B(T)$ and $C(T)$ can be determined from the fitting of magnetization isothermal data. It can be seen from the inset of Fig. 3 that the parameter $A(T)$ varies from negative to positive values around the transition point T_C, and the temperature just corresponding to the zero value of parameter A is consistent with the T_C. In addition, the landau parameter $B(T)$ is observed to be negative below T_C and positive above T_C. This change from negative to positive suggests that the phase transition in the sample is of second order.[58]

In the frame of the Landau theory, the magnetic entropy is obtained from differentiation of the free energy with respect to temperature as:[59]

$$S_M(T,H) = -\left(\frac{G(H,T)}{T}\right) = -\frac{1}{2}A'(T)M^2 - \frac{1}{4}B'(T)M^4 - \frac{1}{6}C'(T)M^6 \quad (10)$$

we notice that $A'(T)$, $B'(T)$ and $C'(T)$ have usually been known as the temperature derivatives of the landau coefficients in eqn (9). The same result is obtained using the equation of state and integration of Maxwell relations. The variation of the experimental and the calculated temperature dependence of the ($-\Delta SM-\Delta S_M(T,\mu_0 H)$) at an applied magnetic fields of 1 T using the eqn (10) for $La_{0.7}Ca_{0.1}Pb_{0.2}Mn_{0.9}Al_{0.05}Sn_{0.05}O_3$ sample is plotted in Fig. 3. Our observation suggests

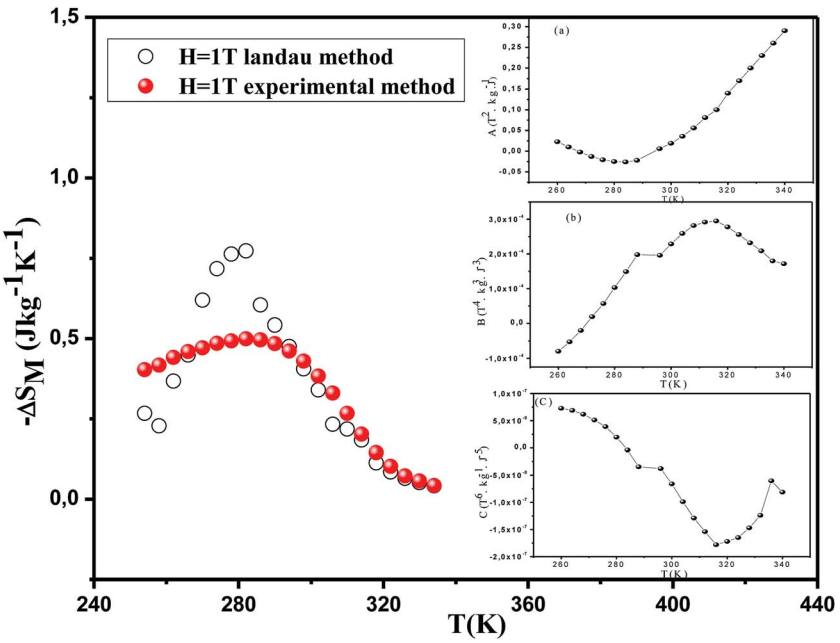

Fig. 3 Experimental and calculated values of the magnetic entropy change *vs.* temperature used the Landau theory under applied magnetic field of 1 T for the $La_{0.7}Ca_{0.1}Pb_{0.2}Mn_{0.9}Al_{0.05}Sn_{0.05}O_3$ compound. The inset: (a)–(c): variation of Landau parameters *A*, *B* and *C* as a function of temperature of $La_{0.7}Ca_{0.1}Pb_{0.2}Mn_{0.9}Al_{0.05}Sn_{0.05}O_3$.

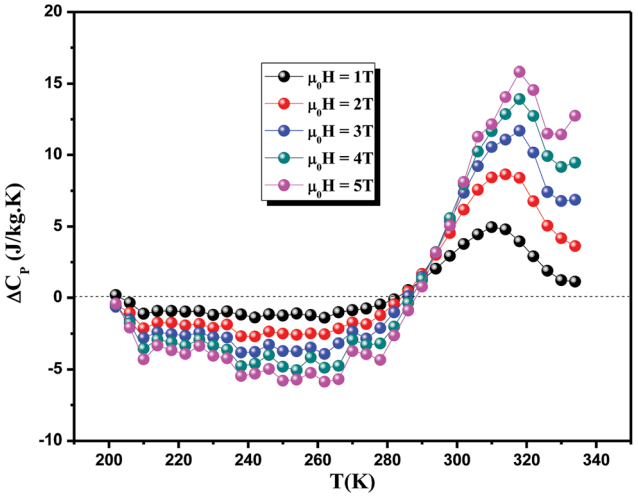

Fig. 4 Change of specific heat of the sample as a function of temperature at different magnetic fields for $x = 0.05$.

that there is a deviation between the experimental and the theoretical data, considering the fact that the magnetoelastic coupling and electron interaction do not directly contribute to the magnetic entropy since the theoretical and experimental curves are not completely confused. It can be attributed to some other factors which have major effects on the magnetic properties of manganites such as the Jahn–Teller effect, exchange interactions and micromagnetism.[60] Such results indicate that the magnetoelastic coupling, which is the interaction between the magnetization and the strain of a magnetic material, and electron interaction have strong influence in determining the magnetocaloric effect.[61–63]

The change of specific heat (ΔC_p) associated with a magnetic field from 0 to $\mu_0 H$ is given by

$$\Delta C_p(T, \mu_0 H) = C_p(T, \mu_0 H) - C_p(T, 0) = -T \frac{\partial \Delta S_M(T, \mu_0 H)}{\partial T} \quad (11)$$

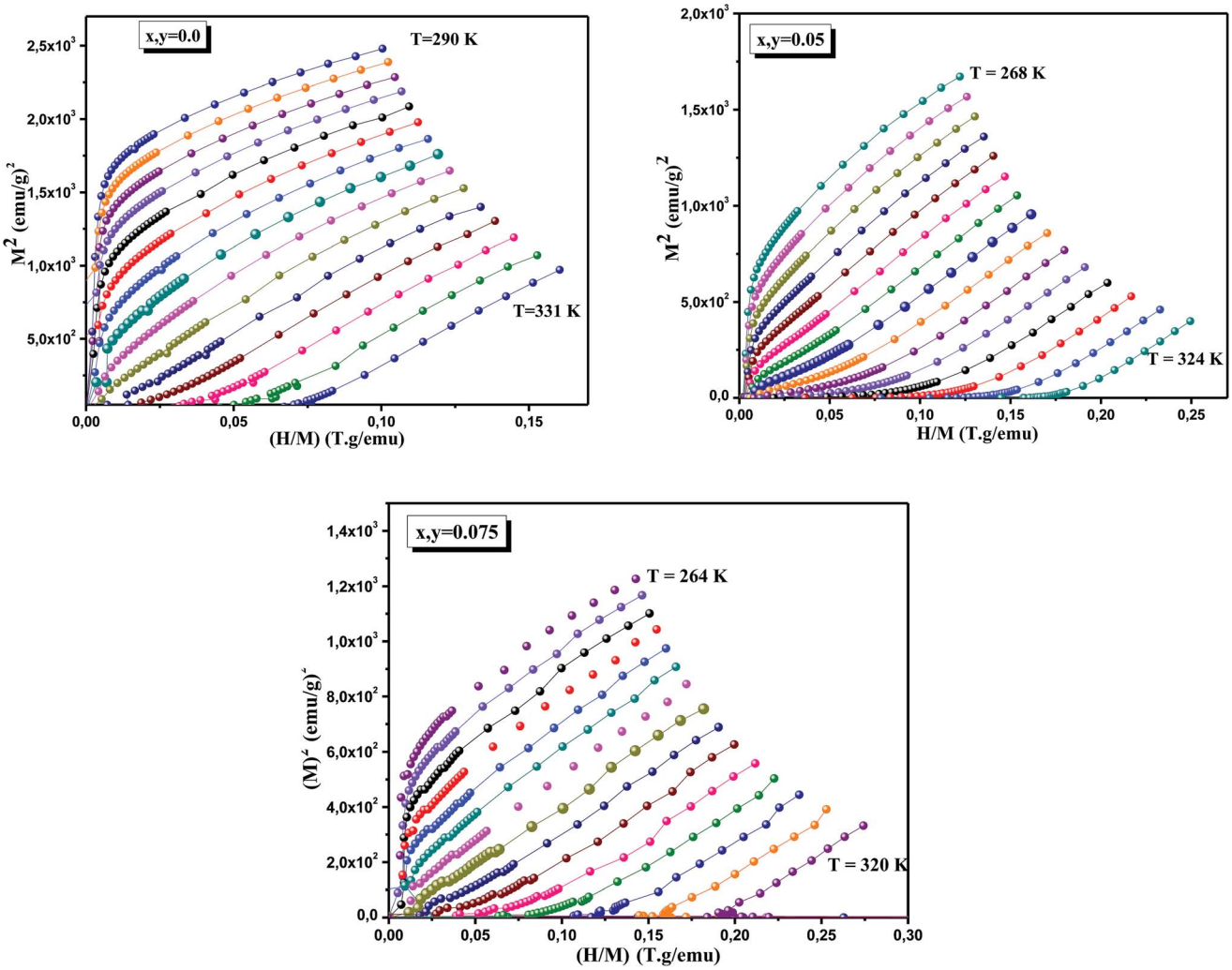

Fig. 5 Arrott plots around T_C for $La_{0.7}Ca_{0.1}Pb_{0.2}Mn_{1-x-y}Al_xSn_yO_3$ ($x, y = 0.0$, 0.05 and 0.075) samples. According to the mean field model, values of critical exponents $\beta = 0.5$ and $\gamma = 1$ should generate the regular Arrott plots, M^2 *vs.* $\mu_0 H/M$.

We have plotted $\Delta C_p(T,\mu_0H)$ *versus* temperature for $x, y = 0.05$ sample at different magnetic field in Fig. 4 calculated from the $(-\Delta S_M)$ by using eqn (11). It shows the presence of anomalies in all curves around T_C due to the magnetic phase transition. In fact, the value of ΔC_p undergoes a sudden change from negative to positive around the Curie point with a negative value below T_C and a positive value above T_C. Furthermore, the maximum/minimum values of ΔC_p increases with the applied magnetic field. The sum of the two parts is the magnetic contribution to the total specific heat which affects the heating or cooling power of the magnetic refrigerator.[64] Moreover, other structural, magnetic and magnetocaloric properties are previously studied.[42]

4.2. Critical behavior

Nowadays, there is a need to design new magnetic systems with a second order transition, low hysteresis losses and attractive RCP values to be compatible for the magnetic freezers. In order to determine the type of magnetic phase transition (first or second order) for our samples in vicinity of Curie temperature, the regular Arrott plot displayed as $M^{1/\beta}$ with respect to $(\mu_0H/M)^{1/\gamma}$, β and γ are the mean field exponents of ($\beta = 0.5$, $\gamma = 1$), are constructed (Fig. 5). A rough determination of the order of magnetic phase transitions is possible by applying the Banerjee criterion, in which the sign of the isotherms slope of M^2 *versus* μ_0H/M will give the nature of the phase transition: positive slope in the high field region indicates absolutely a second order transition, but a negative slope of M^2 *vs.* μ_0H/M reflects that the magnetic system exhibits a first order transition.[65–67] In the present case, all the M^2 *vs.* μ_0H/M curves exhibit a positive slope indicating that the transition between the ferromagnetic and paramagnetic phases is of the second order, according to the criterion proposed by Banerjee.[68] We believe that the substitution of Al^{3+} and Sn^{4+} (nonmagnetic ions) into the Mn site changes structural parameters, such as the bond length ⟨Mn–O⟩ and bond angle ⟨Mn–O–Mn⟩, and dilute the FM lattice. Along these lines, the variation of these factors acts as a fluctuation, and thus influences the FM-interaction strength of DE Mn^{3+}–Mn^{4+} pairs as well as the phase-transition type. The appearance of the second-order magnetic phase transition in LCPMAlSnO is thus understandable. According to mean-field theory, near T_C these curves should show a series of straight lines for different temperatures

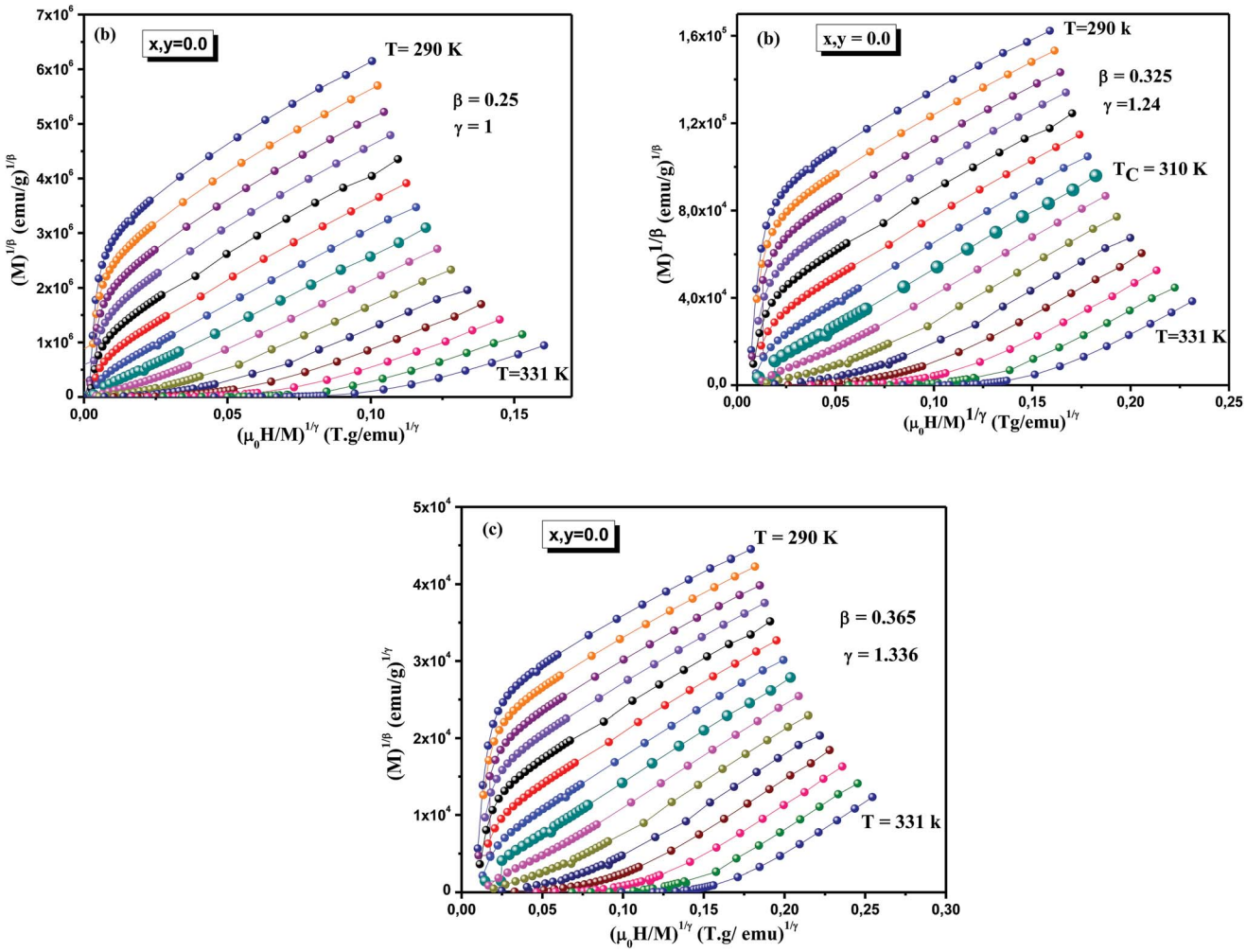

Fig. 6 Modified Arrott plots: $M^{1/\beta}$ *versus* $(\mu_0H/M)^{1/\gamma}$ with (a) tricritical mean-field model ($\beta = 0.25$, $\gamma = 1$), (b) 3D-Ising model ($\beta = 0.325$, $\gamma = 1.24$) and (c) 3D-Heisenberg model ($\beta = 0.365$, $\gamma = 1.336$).

and the line $T = T_C$ should cross the origin.[69] In present study, it is evident in Fig. 5 that these conditions are more accurate for $x, y = 0.05$ and 0.075 samples. In particular, the line of M^2 *vs.* μ_0H/M crosses the origin at T_C = 295 K and 290 K *vs.* (μ_0H/M). This indicates that the mean field model is the best one for the critical analysis of these compounds. As against, for $x, y = 0.0$ sample, the curves in the Arrott plot are nonlinear and show a downward curvature even at a high field region indicating that the exponents with $\beta = 0.5$ and $\gamma = 1$ cannot be used to describe the critical behavior in these samples. In order to analyze more carefully the nature of the magnetic phase transition in $La_{0.7}Ca_{0.1}Pb_{0.2}Mn_{1-x-y}Al_xSn_yO_3$ (x, y = 0.0, 0.05 and 0.075) samples, we realized the studies of the critical behavior near T_C.

The analysis of Arrott plots show that $x, y = 0.05$ and 0.075 samples may be described by the mean field model with $\beta = 0.5$ and $\gamma = 1$. Therefore, to better obtain the right values of β and γ exponents, the data was analyzed using a modified Arrott-plot expression, based on the Arrott–Noakes equation of state:[70]

$$(\mu_0H/M)^{1/\gamma} = a(T - T_C)/T + bM^{1/\beta} \quad (12)$$

where a and b are considered to be constants (in the mean-field theory, values of $\beta = 0.5$ and $\gamma = 1$ should generate the regular Arrott plots, M^2 *vs.* μ_0H/M).

Fig. 6 shows the plot of $M^{1/\beta}$ *versus* $(\mu_0H/M)^{1/\gamma}$ at several temperature by using different models of critical exponents for $La_{0.7}Ca_{0.1}Pb_{0.2}Mn_{1-x-y}Al_xSn_yO_3$ (x, y = 0.0) sample: Fig. 6(a) tricritical mean-Field model ($\beta = 0.25$ and $\gamma = 1$). Fig. 6(b) 3D-Ising model ($\beta = 0.325$ and $\gamma = 1.24$) and Fig. 6(c) 3D-Heisenberg model ($\beta = 0.365$ and $\gamma = 1.336$).

Due to the resemblance of quasi straight lines in the high-field region for each corresponding curve models cited earlier, it seems difficult to fix on which model is the most proper to find out the critical exponents. In order to distinguish which the best model that describes our system, it is necessary to take into account a new indicator for selection. Thus, to confirm the better model to fit our experimental data, their relative slopes (RS) were calculated at the critical point, defined as:

$$\mathrm{RS} = S(T)/S(T_C)$$

where $S(T)$ and $S(T_C)$ are the slopes deduced from MAP around and at T_C respectively. If the MAP shows a series of parallel lines, the relative slope of the most satisfactory model should be kept to 1 regardless temperature. Fig. 7 shows the RS *vs.* T curve ($x, y = 0.0$ and 0.05) for the different models. As shown in Fig. 7, the RS of $La_{0.7}Ca_{0.1}Pb_{0.2}Mn_{1-x-y}Al_xSn_yO_3$ (x, y = 0.0) using mean-field, 3D-Heisenberg and tricritical mean-field model clearly deviates from RS = 1, as against, the RS of 3D-Ising model is close to it. So, it is the best model that can describe these compounds. On the other hand, we noted that the RS of $La_{0.7}Ca_{0.1}Pb_{0.2}Mn_{1-x-y}Al_xSn_yO_3$ (x, y = 0.05 and 0.075) is very close to 1 when using the mean-field model. Therefore, the critical properties of $La_{0.7}Ca_{0.1}Pb_{0.2}Mn_{1-x-y}Al_xSn_yO_3$ ($x, y = 0.0$) and $La_{0.7}Ca_{0.1}Pb_{0.2}Mn_{1-x-y}Al_xSn_yO_3$ (x, y = 0.05 and 0.075) samples can be described with the 3D-Ising model and mean-field model one respectively.

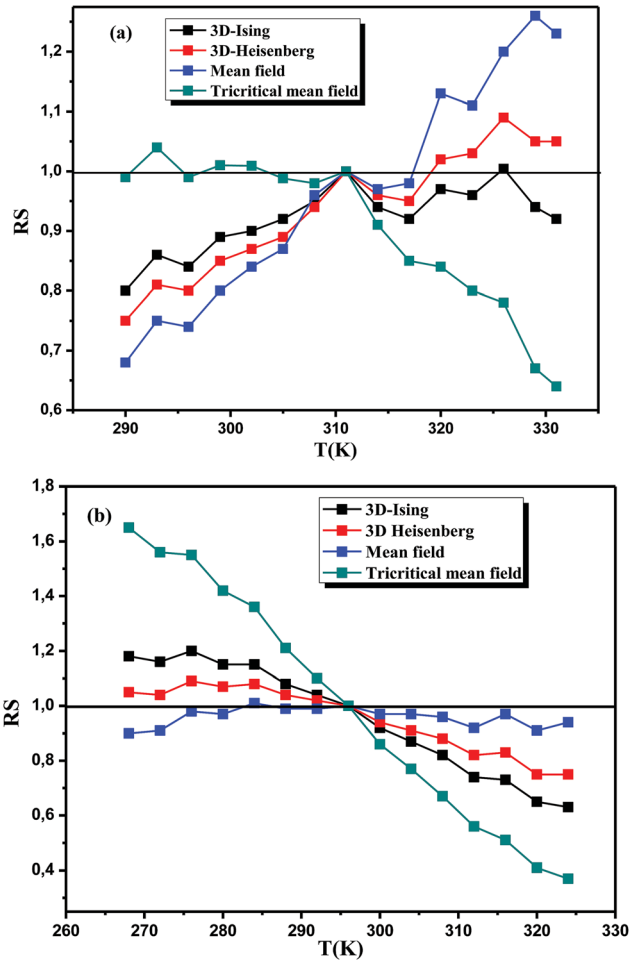

Fig. 7 Relative slope (RS) as a function of temperature of $La_{0.7}Ca_{0.1}Pb_{0.2}Mn_{0.9}Al_{0.05}Sn_{0.05}O_3$, (a) for $x, y = 0.0$ and (b) for $x, y = 0.05$.

According to the modified Arrott plots, we could calculate the values of the spontaneous magnetization $M_S(T)$ and the inverse of susceptibility $\chi_0^{-1}(T)$. Therefore, the linear extrapolation of the high-field straight-line portion of the isotherm provides the values of MS and χ_0^{-1} as an intercept on the $M^{1/\beta}$ and the $(\mu_0H/M)^{1/\gamma}$ axis, respectively. Temperature dependence of the spontaneous magnetization $M_S(T)$ and the inverse susceptibility $\chi_0^{-1}(T)$ for all compounds obtained from the MAP are shown in Fig. 8. The continuous curves denote the power-law fitting of $M_S(T,0)$ and $\chi_0^{-1}(T,0)$ according to eqn (1) and (2), respectively. Thus, new values of the critical exponents and the Curie temperature associated are also mentioned in the same figure and reported in Table 2 for all samples.

Alternatively, a more accurate method to determine the critical exponents β and γ are estimated by the Kouvel–Fisher (KF) method.[71] The K–F method is based on the following equations:

$$\frac{M_S(T)}{dM_S(T)/dT} = \frac{T - T_C}{\beta} \quad (13)$$

$$\frac{\chi_0^{-1}(T)}{d\chi_0^{-1}(T)/dT} = \frac{T - T_C}{\gamma} \quad (14)$$

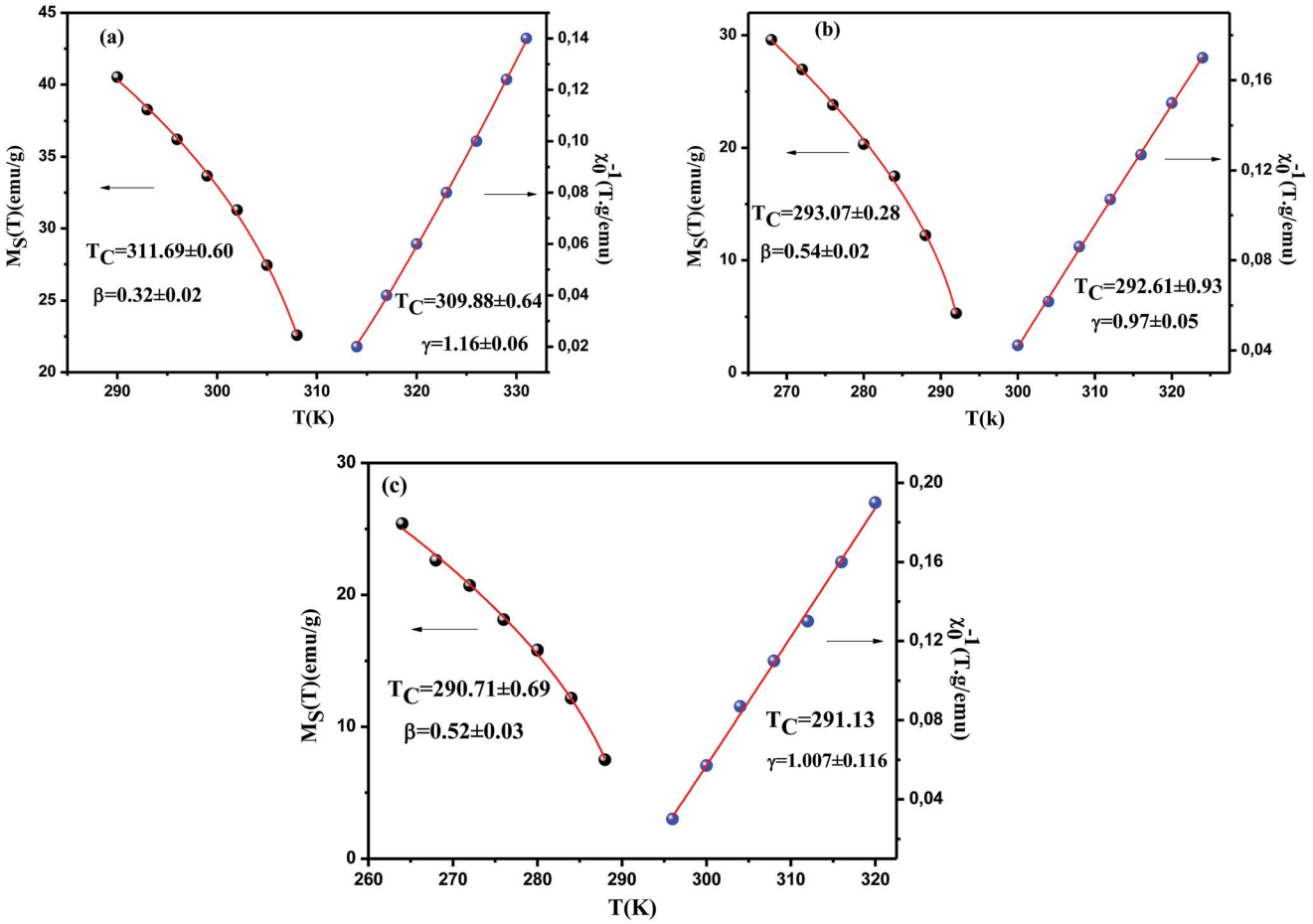

Fig. 8 The spontaneous magnetization $M_S(T, 0)$ (left) and the inverse initial susceptibility $\chi_0^{-1}(T)$ (right) as a function of temperature of $La_{0.7}Ca_{0.1}Pb_{0.2}Mn_{0.9}Al_{0.05}Sn_{0.05}O_3$, (a) for $x, y = 0.0$, (b) for $x, y = 0.05$ and $x, y = 0.075$.

According to this method, the quantities $M_S(T)(dM_S(T)/dT)^{-1}$ and $\chi_0^{-1}(T)(d\chi_0^{-1}(T)/dT)^{-1}$ plotted against temperature in Fig. 9, yield straight lines with slopes $1/\beta$ and $1/\gamma$, respectively, and the intercepts on the T axis of the extrapolation of these straight lines to the ordinate equal to zero gives the values of T_C. From the linear fit to the plots

Table 2 Comparison of critical exponents of $La_{0.7}Ca_{0.1}Pb_{0.2}Mn_{1-x-y}Al_xSn_yO_3$ ($x, y = 0.0$, 0.05 and 0.075) with other reports and various theoretical models

Samples	Techniques	T_C (K)	β	γ	δ	Ref.
$La_{0.7}Ca_{0.1}Pb_{0.2}MnO_3$	MAP	311.69 ± 0.60	0.32 ± 0.02	1.16 ± 0.06	4.63	This work
	KF	312.25 ± 0.82	0.33 ± 0.02	1.20 ± 0.05		
$La_{0.7}Ca_{0.1}Pb_{0.2}Mn_{0.9}Al_{0.05}Sn_{0.05}O_3$	MAP	293.07 ± 0.28	0.54 ± 0.02	0.97 ± 0.05	2.66	This work
	KF	293.46 ± 0.61	0.57 ± 0.02	0.95 ± 0.04		
$La_{0.7}Ca_{0.1}Pb_{0.2}Mn_{0.85}Al_{0.075}Sn_{0.075}O_3$	MAP	290.71 ± 0.69	0.52 ± 0.03	1.007 ± 0.116	3.3	This work
	KF	290.76 ± 0.55	0.50 ± 0.02	1.15 ± 0.14		
Mean field model	Theory	—	0.5	1	3	81
3D-Ising mode	Theory	—	0.325	1.24	4.82	81
Tricritical mean field model	Theory	—	0.25	1	5	82
3D-Heseinberg model	Theory	—	0.365	1.336	4.8	32
$Pr_{0.67}Ba_{0.33}Mn_{0.95}Fe_{0.05}O_3$		128	0.5 ± 0.026	1.007 ± 0.002	2.920	74
$La_{0.7}Ca_{0.2}Sr_{0.1}MnO_3$		289	0.26	1.06	5.1	75
$La_{0.67}Pb_{0.33}MnO_3$		360.41	0.367	1.22	4.29	76
$LaMn_{0.9}Ti_{0.1}O_3$		145.3 ± 0.1	0.375 ± 0.00	1.25 ± 0.02	4.11	77
$Nd_{0.7}Pb_{0.3}MnO_3$		148	0.361 ± 0.001	1.325 ± 0.001	4.62	78
$TbCo_{1.9}Fe_{0.1}$		303	0.541 ± 0.001	1.023 ± 0.002	2.75	79
$La_{0.7}Sr_{0.3}MnO_3$		360	0.45 ± 0.02	1.08 ± 0.04	3.04	80

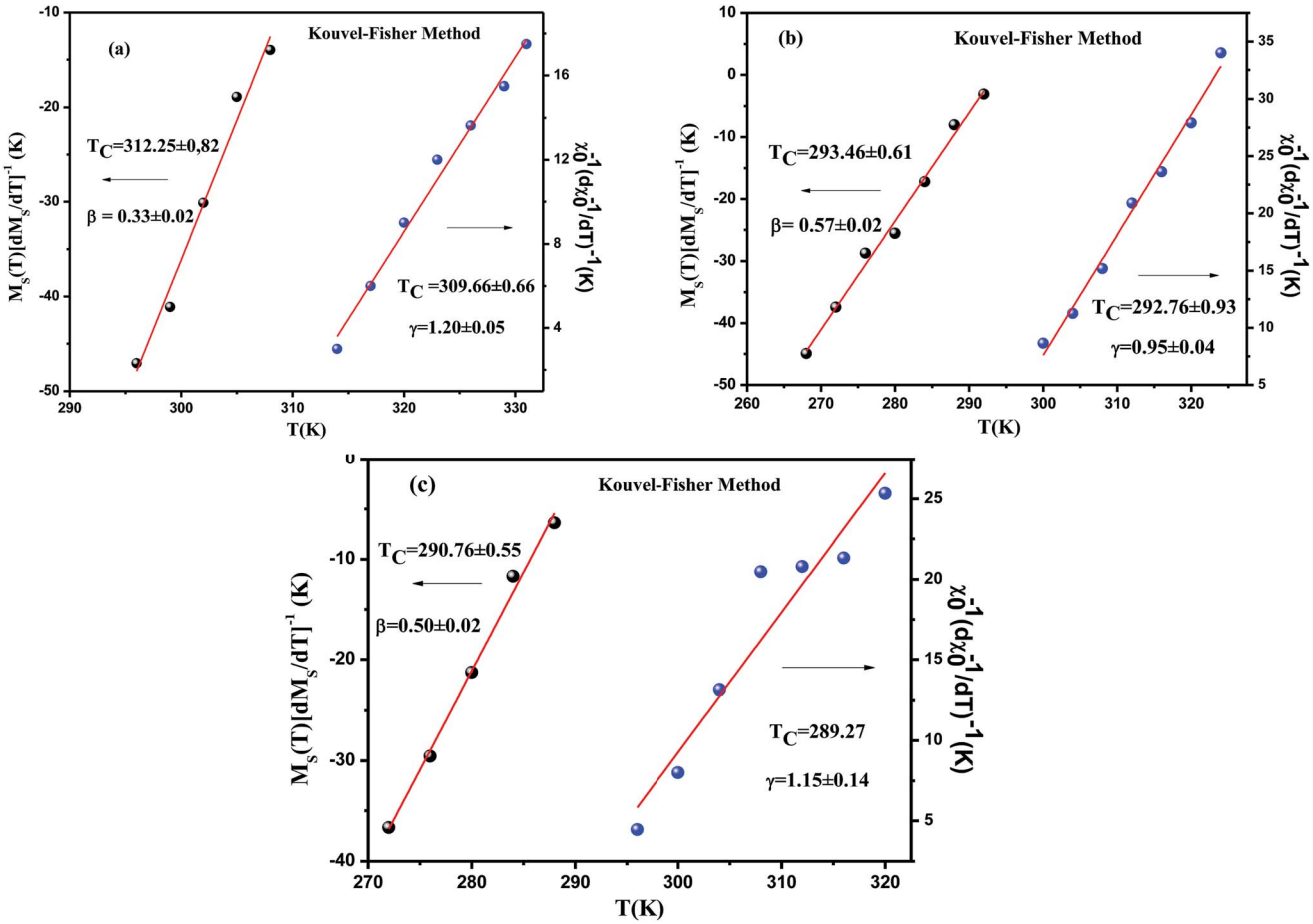

Fig. 9 Kouvel–Fisher plots for the spontaneous magnetization $M_S(T)$ and the inverse initial susceptibility $\chi_0^{-1}(T)$ for $La_{0.7}Ca_{0.1}Pb_{0.2}MnO_3$ (a), $La_{0.7}Ca_{0.1}Pb_{0.2}Mn_{0.9}Al_{0.05}Sn_{0.05}O_3$ (b) and $La_{0.7}Ca_{0.1}Pb_{0.2}Mn_{0.9}Al_{0.075}Sn_{0.075}O_3$ (c). Solid lines correspond to the linear fit of $M_S(T)$ and $\chi_0^{-1}(T)$ curves with eqn (14) and (15), respectively.

following the KF method, we have obtained the critical exponents.

For $x, y = 0.0$ sample,

$$\left\{\begin{array}{ll} \beta = 0.33 \pm 0.02 & \text{with} \quad T_C = 312.25 \pm 0.82 \\ \gamma = 1.20 \pm 0.05 & \text{with} \quad T_C = 309.66 \pm 0.66 \end{array}\right\},$$

For $x, y = 0.05$ sample,

$$\left\{\begin{array}{ll} \beta = 0.57 \pm 0.02 & \text{with} \quad T_C = 293.46 \pm 0.61 \\ \gamma = 0.95 \pm 0.04 & \text{with} \quad T_C = 292.76 \pm 0.93 \end{array}\right\}$$

and

For $x, y = 0.075$ sample,

$$\left\{\begin{array}{ll} \beta = 0.50 \pm 0.02 & \text{with} \quad T_C = 290.76 \pm 0.55 \\ \gamma = 1.15 \pm 0.14 & \text{with} \quad T_C = 289.27 \end{array}\right\}$$

Obviously, it is clearly remarked that these values are also in agreement with those obtained from modified Arrot plots (MAP). This confirms that the estimated values of the critical exponents are self-consistent and unambiguous. Besides, concerning the final parameter δ, it can be determined directly using the isothermal magnetization $M(\mu_0 H)$ at TC (see in Fig. 10). The inset of the same figure shows the $M(\mu_0 H)$ curve on a log–log scale. According to eqn (3), the value of critical exponent δ can be determined directly from the fitting of the high field region of critical isotherm $M(T_C,\mu_0 H)$ on log–log scale as reported in Fig. 10. The obtained value for the currently investigated sample are 4.54, 2.85 and 2.7 for $x, y = 0.0$, 0.05 and 0.075, respectively.

Furthermore, according to the statistical theory, these critical exponents are interrelated and fulfill the Widom scaling law which critical exponents β, γ, and δ are related in following way:[72]

$$\delta = 1 + \frac{\gamma}{\beta} \tag{15}$$

The replacement of β and γ determined by Kouvel–Fisher method in eqn (15) donates 4.63, 2.66 and 3.3 as a value of delta for $x, y = 0.0$, 0.05 and 0.075, respectively, which are so close to those determined by the critical isotherm. This relationship has been tested by plotting $M(T = T_C)$ *versus* $\mu_0 H^{\beta/(\beta+\gamma)} = \mu_0 H^{1/\delta}$ and checking the linearity of the curve as shown in Fig. 11. Hence, we can conclude that the values of different critical exponents and T_C determined for our compounds obey the Widom scaling

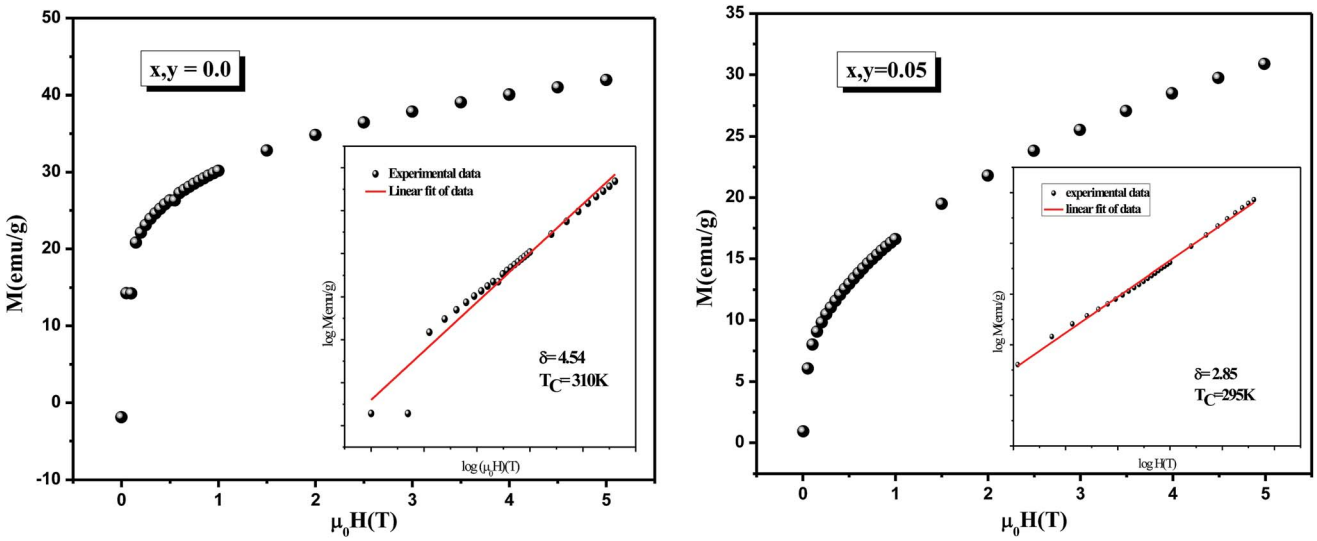

Fig. 10 Critical isotherms of M *versus* $\mu_0 H$ for $La_{0.7}Ca_{0.1}Pb_{0.2}Mn_{1-x-y}Al_xSn_yO_3$ (x, y = 0.0 and 0.05). The inset: shows the log–log scale for M *versus* $\mu_0 H$.

relation, implying that the obtained β and γ values are auspicious.

One can notice that the critical exponents of $La_{0.7}Ca_{0.1}Pb_{0.2}Mn_{1-x-y}Al_xSn_yO_3$ (x, y = 0.0) and $La_{0.7}Ca_{0.1}Pb_{0.2}Mn_{1-x-y}Al_xSn_yO_3$ (x, y = 0.05 and 0.075) samples match well with those of the 3D-Ising and mean-field model respectively. Therefore, it is important to check if these critical exponents can generate the scaling equation of state for these systems.

Using the values of β and γ given by the Kouvel Fisher technique (KF), the scaled data are plotted in Fig. 12. For a more convenient visualization of the results, we represent in the inset the same data in a log–log scale. It is clear that all the magnetization data fall on two individual branches, one for $T < T_C$ and the other for $T > T_C$. This clearly suggests that the values of the exponents and T_C for these samples are reasonably accurate and consistent with the scaling hypothesis. Consequently, the $La_{0.7}Ca_{0.1}Pb_{0.2}Mn_{1-x-y}Al_xSn_yO_3$ samples undergo the second-order magnetic phase transition. Moreover, the reliability of β, δ and T_C can be ascertained by checking the scaling of the magnetization curves. In fact, for magnetic systems, the scaling equation of state takes the form:[69]

$$\frac{\mu_0 H}{M^{\delta}} = h\left(\frac{\varepsilon}{M^{1/\beta}}\right) \tag{16}$$

where $h(x)$ is a scaling function which characterizes the magnetization behavior along coexistence ($\mu_0 H = 0$, $\varepsilon < 0$) and the critical isotherm ($\varepsilon = 0$), respectively. Thus, according to eqn (16), if the appropriate values for the critical exponents and for the Curie temperature are used, the plot of $\frac{M}{(\mu_0 H)^{1/\delta}}$ *vs.* $\frac{\varepsilon}{(\mu_0 H)^{1/\Delta}}$ ($\Delta = \beta + \gamma$), should correspond to a universal curve onto which all experimental data points collapse.[73]

The scaled data are plotted in Fig. 13, using the values of β, γ and T_C obtained from the K–F method, for the x, y = 0.05 sample. The excellent overlap of the experimental data points clearly indicates that the critical parameters obtained for these compounds are in agreement with the scaling hypothesis, which further corroborates the reliability of the obtained critical exponents near magnetic transition.

This shows that the critical parameters determined are in good agreement with the scaling hypothesis, which further corroborates the reliability of the obtained critical exponents.

To put our obtained results in the context of previous works, the values of the critical exponents for our samples derived from various methods and some other manganites reported in literature,[74,80] as well as the theoretical values based on various models,[81,82] are summarized in Table 2 for comparison. Clearly, the data in this table support the conclusion that the critical

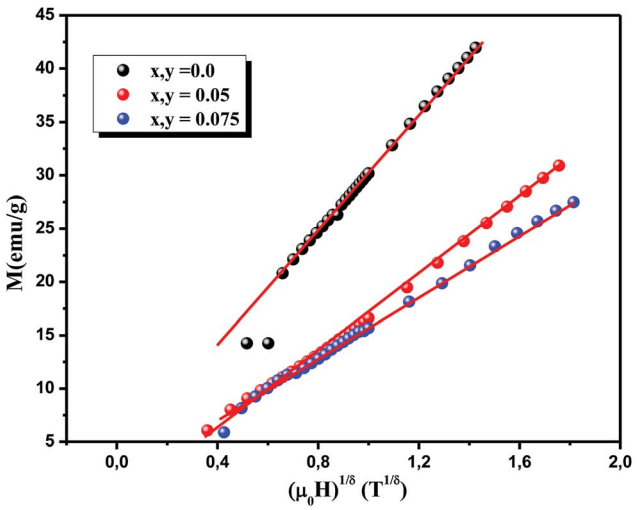

Fig. 11 The linearity of the $M(T = T_C)$ *versus* $\mu_0 H^{\beta/(\beta+\gamma)} = \mu_0 H^{1/\delta}$ curves validates the value of δ calculated using the Widom relationship with the experimental data.

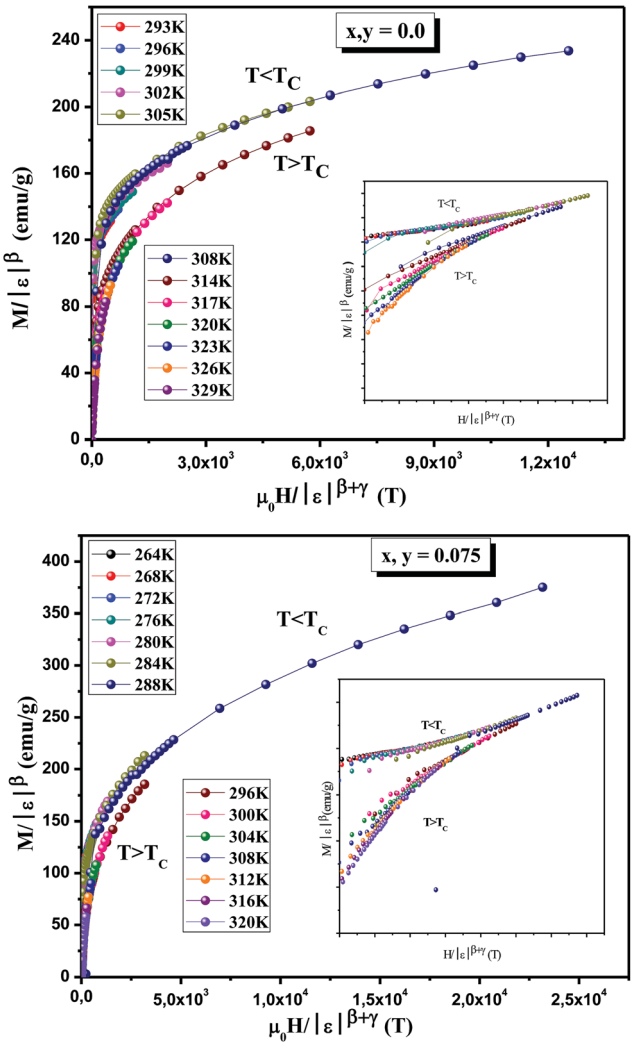

Fig. 12 Scaling plots for $La_{0.7}Ca_{0.1}Pb_{0.2}Mn_{1-x-y}Al_xSn_yO_3$ (x, y = 0.0 and 0.075) below and above T_C using β and γ determined by the Kouvel–Fisher method. The insets show the same plots on a log–log scale.

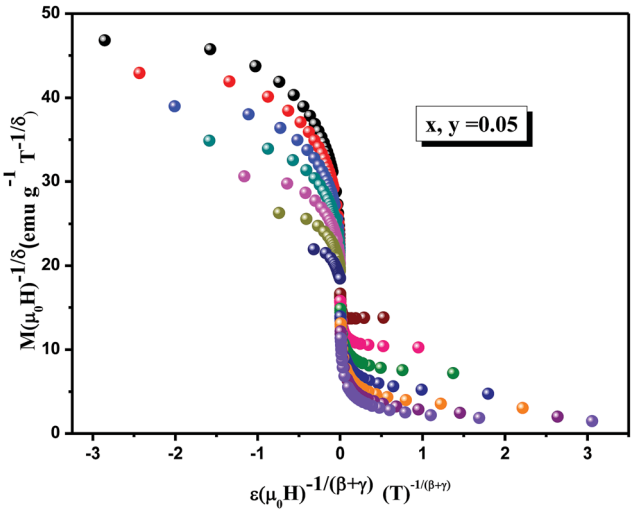

Fig. 13 Normalized isotherms of $La_{0.7}Ca_{0.1}Pb_{0.2}Mn_{0.9}Al_{0.05}Sn_{0.05}O_3$ below and above the Curie temperature using the values of β and Δ determined by the K–F method.

exponents of $La_{0.7}Ca_{0.1}Pb_{0.2}MnO_3$ and $La_{0.7}Ca_{0.1}Pb_{0.2}Mn_{1-x-y}Al_xSn_yO_3$ (x, y = 0.05 and 0.075) are completely agree with those of the 3D-Ising model and the mean field model, respectively. Therefore, it is important to check if these critical exponents can generate the scaling equation of state for these systems.

In order to demonstrate the influence of the critical exponents on the MCE, we analyzed the dependence of the entropy change on the field. According to Oesterreicher *et al.*, for a material displaying a second order phase transition, the field dependence of ΔS_M can be expressed as follows:

$$\Delta S_M = a(\mu_0 H)^n \tag{17}$$

where the exponent n depends on the magnetic state of the compound. It can be locally calculated as follows:

$$n = \frac{d\ln \Delta S_M}{d\ln(\mu_0 H)} \tag{18}$$

The obtained largest values of n approaching to 2 in the paramagnetic range for $T > T_C$, $n = 1$ for $T < T_C$,[42] and at the peak temperatures T_C, the exponent n becomes field independent and is expressed as:[83]

$$n(T_C) = 1 + \frac{\beta - 1}{\beta + \gamma} \tag{19}$$

which can be transformed using the relation $\beta\delta = (\beta + \gamma)$

$$n = 1 + \frac{1}{\delta}\left(1 - \frac{1}{\beta}\right) \tag{20}$$

where β, γ and δ are the critical exponents. Using the values of β and δ, we obtained the values of n which are calculated to be 0.56, 0.62 and 0.69 for x, y = 0.0, 0.05 and 0.075 samples, respectively. Apparently, these values are in good agreement with the mean field prediction n = 2/3 (ref. 84) for x, y = 0.05 and 0.075 samples. On the other hand, for x, y = 0.0 sample, these values are lower. Also, the n values obtained from the power-law fitting of the ΔS_M^{max} *vs.* $\mu_0 H$ curve are higher than those calculated from eqn (20). The deviation from the mean field behavior is due to the presence of local inhomogeneities around the transition temperature.[85]

In the following section, we will use the mean-field theory to study the spontaneous magnetization (M_{spont}) in our samples (x, y = 0.05 and 0.075). A general result issued from a mean-field theory reveals the dependence of the magnetic entropy on the relative magnetization can be described as:[86]

$$S(\sigma) = -NK_B\left[\ln(2J+1) - \ln\left(\frac{\sinh\left(\frac{2J+1}{2J}B_J^{-1}(\sigma)\right)}{\sinh\left(\frac{1}{2J}B_J^{-1}(\sigma)\right)}\right) + B_J^{-1}(\sigma)\sigma\right] \tag{21}$$

where $\sigma = M/g\mu\beta JN$, M is the magnetization, N is the number of spins, J is the spin value, k_B and B_J are the Boltzmann constant

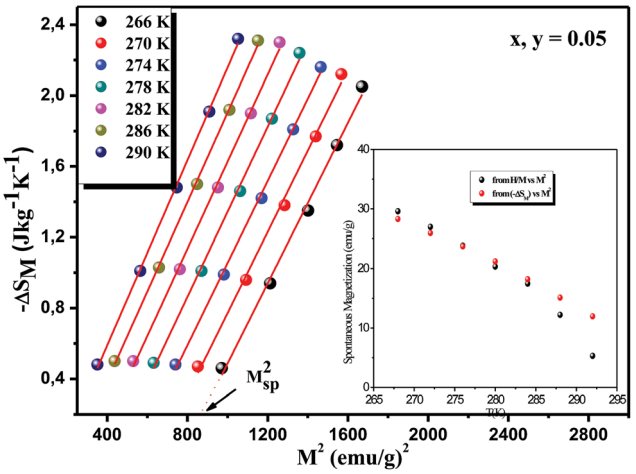

Fig. 14 Isothermal $-\Delta S_M$ *vs.* M^2 curves (the solid lines are linear fits to the data). The inset: spontaneous magnetization of $La_{0.7}Ca_{0.1}Pb_{0.2}Mn_{0.9}Al_{0.05}Sn_{0.05}O_3$ deduced from the extrapolation of the isothermal $-\Delta S_M$ *vs.* M^2 curves and from the Arrott plots $\mu_0 H/M$ *vs.* M^2.

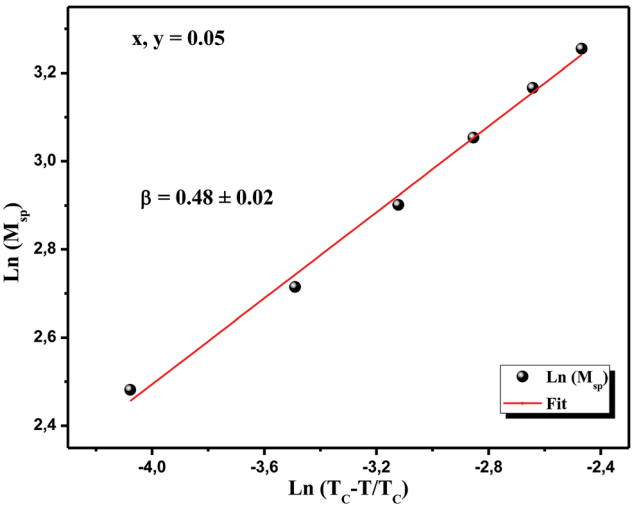

Fig. 15 Ln (M_{Sp}) *vs.* Ln ($T_C - T/T_C$). The red line is the linear fitting.

and the Brillouin function respectively. From a power expansion of eqn (21), ΔS_M is proportional to M^2, from the mean-field model, for small M values:

$$-S(\sigma) = \frac{3J}{2J+1} N k_B \sigma^2 + 0(\sigma^4) \quad (22)$$

However, in ferromagnetic state (bellow T_C) the system has a spontaneous magnetization where $\sigma = 0$ state is never attained. After restriction the first term of eqn (22), the magnetic entropy change can be donated by this equation:

$$-S(\sigma) = \frac{3J}{2J+1} N k_B \left(\sigma^2 - \sigma^2_{spon}\right) \quad (23)$$

Fig. 14 shows the isothermal $-\Delta S$ *vs.* M^2 curves in the ferromagnetic region ($T < T_C$). The isothermal $-\Delta S_M$ *vs.* M^2 plots in the ferromagnetic region, shows an horizontal drift from the origin corresponding to the value of $M_{Sp}{}^2(T)$, whereas the $-\Delta S_M$ *vs.* M^2 plots begin at a null M value for $T > T_C$.[59] The linear dependence of $-\Delta S_M$ on M^2 is clearly shown in Fig. 14 with an approximately constant slope throughout the FM region. In addition, by linearly extending the $-\Delta S$ *vs.* M^2 curves to $-\Delta S = 0$, the values of the spontaneous magnetization M_{Sp} at several temperature have been evaluated. We have compared these results of M_S with the results obtained from the modified Arrott plot as shown in the inset of Fig. 14. As one can see clearly, an excellent agreement between the two methods indicates the validity of this process to estimate the spontaneous magnetization using a mean-field analysis of the magnetic entropy change in $La_{0.7}Ca_{0.1}Pb_{0.2}Mn_{1-x-y}Al_xSn_yO_3$ (x, $y = 0.05$ and 0.075) system.

Interestingly, we can further discuss the feasibility and applicability of the mean field theory applied in the above analysis. The spontaneous magnetization can be fitted by using:

$$M_{Sp}(T) = M_{Sp}(0)\left[1 - \frac{T}{T_C}\right]^{\beta} \quad (24)$$

To determine the value of the critical exponent β, we changed this expression to log–log scale. Fig. 15 shows $\ln(M)$ *vs.* $\ln(T_C - T/T_C)$, the linear fitting gives the value of β to be 0.48 ± 0.017 which is consistent with the standard mean field model ($\beta = 0.5$).

Here we distinguish an excellent agreement between the experimental value ($\beta = 0.48$) and the theoretical value (mean field model, $\beta = 0.5$) allows to confirm the validity of this technique to estimate the spontaneous magnetization using a mean-field procedure of the magnetic entropy change.

5. Conclusion

In the present work, we investigated the magnetic, critical exponents and magnetocaloric properties of polycrystalline $La_{0.7}Ca_{0.1}Pb_{0.2}Mn_{1-x-y}Al_xSn_yO_3$ synthesized by sol–gel method. The values of critical exponents for all samples specimens corresponding to the PM to FM phase transition were extracted using the modified Arrott plot method, Kouvel–Fisher method and critical isotherm analysis. Interestingly, the exponent values founded are so close to values expected for the universality class of 3D-Ising model and mean field model for $x = 0.0$, 0.05 and 0.075 respectively. The validity of the obtained critical exponents using various methods has been confirmed by the Widom scaling relation and universal scaling hypothesis. We can note that the change in the universality class is due to the relevant disorder introduced by the (Al, Sn) doping.

Furthermore, the methodology based on the analysis of the magnetic entropy change (ΔS_M) *vs.* M^2, compared with the classical extrapolation of the Arrott curves ($\mu_0 H/M$ *vs.* M^2), confirms that the magnetic entropy change is a valid method to determine the spontaneous magnetization of the $La_{0.7}Ca_{0.1}Pb_{0.2}Mn_{1-x-y}Al_xSn_yO_3$ system. These exceptional

results have a role to get fruitful investigations and we can confirm that the insight gained from the use of different methodologies for a given magnetic system is very interesting.

Conflicts of interest

There are no conflicts to declare.

References

1 K. A. Gschneidner Jr, V. K. Pecharsky and A. O. Tsokol, *Rep. Prog. Phys.*, 2005, **68**, 1479.
2 N. A. de Oliveira and P. J. vonRanke, *Phys. Rep.*, 2010, **489**, 89.
3 J. Mira, J. Rivas, F. Rivadulla, C. VaHzquez-vaHzquez and M. A. LoHpez-Quintela, *Phys. Rev. B: Condens. Matter Mater. Phys.*, 1999, **60**, 2929.
4 K. Chahara, T. Ohno, M. Kasai and Y. Kosono, *Appl. Phys. Lett.*, 1993, **63**, 1990.
5 R. von Helmolt, J. Weeker, B. Holzapfel, L. Schultz and K. Samwer, *Phys. Rev. Lett.*, 1993, **71**, 2331.
6 M. M. Cormack, S. Jin, T. H. Tiefel, R. M. Fleming, J. M. Phillips and R. Ramesh, *Appl. Phys. Lett.*, 1994, **64**, 3045.
7 S. Jin, T. H. Tiefel, M. Mc Cormack, R. A. Fastnacht, R. Ramesh and L. H. Chen, *Science*, 1994, **264**, 413.
8 W. J. Lu, X. Luo, C. Y. Hao, W. H. Song and Y. P. Sun, *J. Appl. Phys.*, 2008, **104**, 113908.
9 N. S. Bingham, M. H. Phan, H. Srikanth, M. A. Torija and C. Leighton, *J. Appl. Phys.*, 2009, **106**, 023909.
10 A. N. Ulyanov, J. S. Kim, G. M. Shin, Y. M. Kang and S. I. Yoo, *J. Phys. D: Appl. Phys.*, 2007, **40**, 123.
11 P. Nisha, S. S. Pillai, A. Darbandi, A. Misra, K. G. Suresh, M. R. Varma and H. Hahn, *J. Phys. D: Appl. Phys.*, 2010, **43**, 135001.
12 W. Tang, W. Lu, X. Luo, B. Wang, X. Zhu, W. Song, Z. Yang and Y. Sun, *J. Magn. Magn. Mater.*, 2010, **322**, 2360.
13 M. Khlifi, M. Bejar, O. EL Sadek, E. Dhahri, M. A. Ahmed and E. K. Hlil, *J. Alloys Compd.*, 2011, **509**, 7410.
14 J. B. Goodenough, *J. Appl. Phys.*, 1997, **81**, 5330.
15 A. J. Millis, B. I. Shraiman and R. Mueller, *Phys. Rev. Lett.*, 1996, **77**, 175.
16 C. Zener, *Phys. Rev.*, 1951, **82**, 403.
17 J. Dhahri, A. Dhahri, M. Oummezzine and E. K. Hlil, *J. Magn. Magn. Mater.*, 2015, **378**, 353–357.
18 C. V. Mohan, M. Seeger, H. Kronmüller, P. Murugaraj and J. Maier, *J. Magn. Magn. Mater.*, 1998, **83**, 348.
19 S. Nair, A. Banerjee, A. V. Narlikar, D. Prabhakaran and A. T. Boothroyd, *Phys. Rev. B*, 2003, **68**, 132404.
20 K. Ghosh, C. J. Lobb, R. L. Greene, S. G. Karabashev, D. A. Shulyatev, A. A. Arsenov and Y. Mukovskii, *Phys. Rev. Lett.*, 1998, **81**, 4740.
21 N. Mautis, I. Panagiotopoulos, M. Pissas and D. Niarchos, *Phys. Rev. B: Condens. Matter Mater. Phys.*, 1999, **59**, 1129.
22 M. Oumezzine, O. Peña, S. Kallel and S. Zemni, *Solid State Sci.*, 2011, **13**, 1829–1834.
23 T. L. Phan, S. G. Min, S. C. Yu and S. K. Oh, *J. Magn. Magn. Mater.*, 2006, **304**, 778.
24 M. Ziese, *J. Phys. Condens. Matter*, 2001, **13**, 2919.
25 M. H. Phan, V. Franco, N. S. Bingham, H. Srikanth, N. H. Hur and S. C. Yu, *J. Alloys Compd.*, 2010, **508**, 238.
26 S. Roler, U. K. Roler, K. Nenkov, D. Eckert, S. M. Yusuf, K. Korr and K. H. Muller, *Phys. Rev. B: Condens. Matter Mater. Phys.*, 2004, **70**, 104417.
27 A. Berger, G. Camopillo, P. Vivas, J. E. Pearson, S. D. Bader, E. Baca and P. Prieto, *J. Appl. Phys.*, 2002, **91**, 8393.
28 J. Yang and Y. P. Lee, *Appl. Phys. Lett.*, 2007, **91**, 142512.
29 J. Yang, Y. P. Lee and Y. Li, *Phys. Rev. B: Condens. Matter Mater. Phys.*, 2007, **76**, 054442.
30 R. S. Freitas, C. Haetinger, P. Pureur, J. A. Alonso and L. Ghivelder, *J. Magn. Magn. Mater.*, 2001, **226–230**, 569.
31 M. Seeger, S. N. Kaul, H. Kronmüller and R. Reisser, *Phys. Rev. B: Condens. Matter Mater. Phys.*, 1995, **51**, 12585.
32 J. L. Alonso, L. A. Fernández, F. Guinea, V. Laliena and V. Martín-Mayor, *Nucl. Phys. B*, 2001, **596**, 587.
33 M. Kar, A. Perumal and S. Ravi, *Phys. Status Solidi B*, 2006, **243**, 1908.
34 A. Olega, A. Salazar, D. Prabhakaran and A. T. Boothroyd, *Phys. Rev. B: Condens. Matter Mater. Phys.*, 2004, **70**, 184402.
35 Ma. Oumezzine, O. Peña, S. Kallel and M. Oumezzine, *J. Alloys Compd.*, 2012, **539**, 116.
36 Ma. Oumezzine, O. Peña, S. Kallel and S. Zemni, *J. Solid State Sci.*, **13**(2011), 1829.
37 P. Nisha, S. S. Pillai, K. G. Suresh and M. R. Varma, *Solid State Sci.*, 2012, **14**, 40–47.
38 A. Dhahri, J. Dhahri, E. K. Hlil and E. Dhahri, *J. Alloys Compd.*, 2012, **530**, 1–5.
39 K. Ghosh, C. J. Lobb, R. L. Greene, S. G. Karabashev, D. A. Shulyatev, A. A. Arsenov and Y. Mukovskii, *Phys. Rev. Lett.*, 1998, **81**, 4740.
40 J. S. Amaral and V. S. Amaral, *J. Magn. Magn. Mater.*, 2010, **322**, 1552.
41 S. Nair, A. Banerjee, A. V. Narlikar, D. Prabhakaran and A. T. Boothroyd, *Phys. Rev. B: Condens. Matter Mater. Phys.*, 2003, **68**, 132404.
42 K. Dhahri, N. Dhahri, J. Dhahri, K. Taibi and E. K. Hlil, *J. Alloys Compd.*, 2017, **699**, 619–626.
43 H. E. Stanley, *Rev. Mod. Phys.*, 1999, **71**, 358.
44 S. N. Kaul, *J. Magn. Magn. Mater.*, 1985, **53**, 5.
45 E. Tka, K. Cherif and J. Dhahri, *Appl. Phys. A*, 2014, **116**, 1181–1191.
46 E. Tka, K. Cherif, J. Dhahri and E. Dhahri, *J. Alloys Compd.*, 2011, **509**, 8047–8055.
47 Za. Mohamed, M. Abassi, E. Tka, J. Dhahri and E. K. Hlil, *J. Alloys and Compds*, 2015, **646**, 23–31.
48 V. K. Pecharsky, K. A. Gschneidner and A. O. Tsokol, *Reports on Progress in Physics*, 2005, **68**, 1479.
49 D. T. Morelli, A. M. Mance, J. V. Mantese and A. L. Micheli, *J. Appl. Phys.*, 1996, **79**, 373.
50 V. K. Pecharsky and K. A. Gschneidner Jr, *Phys. Rev. Lett.*, 1997, **78**, 4494.
51 D. N. H. Nam, N. V. Dai, L. V. Hong, N. X. Phyc, S. C. Yu, M. Tachibana and E. Takayama-Muromachi, *J. Appl. Phys.*, 2008, **103**, 043905.

52 D. T. Morelli, A. M. Mance, J. V. Mantese and A. L. Micheli, *J. Appl. Phys.*, 1996, **79**, 373.
53 Y. Sun, M. B. Salamon and S. H. Chun, *J. Appl. Phys.*, 2002, **92**, 3235.
54 X. Bohigas, J. Tejada, E. Del Barco, X. X. Zhang and M. Sales, *Appl. Phys. Lett.*, 1998, **73**, 390.
55 N. Chau, H. N. Nhat, N. H. Luong, D. L. Minh, N. D. Tho and N. N. Chau, *Phys. B*, 2003, **327**, 270.
56 V. A. Amaral and J. S. Amaral, *J. Magn. Magn. Mater.*, 2004, **272**, 2104.
57 J. S. Amaral, M. S. Reis, V. A. Amaral, T. M. Mendonca, J. P. Araúji, M. A. Sà, P. B. Tvares and J. M. Vieira, *J. Magn. Magn. Mater.*, 2005, **290**, 686.
58 M. S. Anwar, S. Kumar, F. Ahmed, N. Arshi, G. W. Kim and B. H. Koo, *J. Korean Phys. Soc.*, 2012, **60**, 1587.
59 M. S. Anwar, S. Kumar, F. Ahmed, N. Arshi, G. W. Kim and B. H. Koo, *J. Korean Phys. Soc.*, 2012, **60**, 1587.
60 H. Yang, P. Zhang, Q. Wu, H. Ge and M. pan, *J. Magn. Magn. Mater.*, 2012, **324**, 3727.
61 R. Venkatesh, M. Pattabiraman, K. Sethupathi, G. Rangarajan, S. Angappane and J.-G. Park, *J. Appl. Phys.*, 2008, **103**, 07B319. 17.
62 S. Das and T. K. Dey, *J. Phys.: Condens. Matter*, 2006, **18**, 7629.
63 V. S. Amaral and J. S. Amaral, *J. Magn. Magn. Mater.*, 2004, **272–276**, 2104.
64 H. Yang, Y. H. Zhu, T. Xian and J. L. Jiang, *J. Alloys Compd*, 2013, **555**, 150.
65 A. V. Deshmukh, S. I. Patil, S. M. Bhagat, P. R. Sagdeo, R. J. Choudhary and D. M. Phase, *J. Phys. D: Appl. Phys.*, 2009, **42**, 185410.
66 P. Dey and T. K. Nath, *Phys. Rev. B: Condens. Matter Mater. Phys.*, 2006, **73**, 214425.
67 H. J. Blythe and V. M. Fedosyuk, *J. Phys.: Condens. Matter*, 1995, **7**, 3461.
68 B. K. Banerjee, *Phys. Lett.*, 1964, **12**, 16.
69 H. E. Stanley, *Introduction to Phase Transitions and Critical Phenomena*, Oxford University Press, London, 1971.
70 A. Arrott and J. E. Noakes, *Phys. Rev. Lett.*, 1967, **19**, 786.
71 J. S. Kouvel and M. E. Fisher, *Phys. Rev.*, 1964, **136**, A1626.
72 B. Widom, Degree of the critical isotherm, *J. Chem. Phys.*, 1964, **41**, 1633.
73 R. M'nassri, N. ChnibaBoudjada and A. Cheikhrouhou, *J. Alloys Compd*, 2015, **640**, 183.
74 M. Baazaoui, Sobhi Hcini, Michel Boudard, Sadok Zemni and Mohamed Oumezzine, *J. Magn. Magn. Mater.*, 2016, **401**, 323–332.
75 M. H. Phan, V. Franco, N. S. Bingham, H. Srikanth, N. H. Hur and S. C. Yu, *J. Alloy. Comp*, 2010, **508**, 238.
76 N. Dhahri, J. Dhahri, E. K. Hlil and E. Dhahri, *J. Magn. Magn. Mater.*, 2012, **324**, 806.
77 J. Yang and Y. P. Lee, *Appl. Phys. Lett.*, 2007, **91**, 142512.
78 N. Ghosh, S. Rößler, U. K. Rößler, K. Nenkov, S. Elizabeth, H. L. Bhat, K. Dörr and K. H. Müller, *J. Phys.: Condens. Matter*, 2006, **18**, 557.
79 M. Halder, S. M. Yusuf and M. D. Mukada, *Phys. Rev. B: Condens. Matter Mater. Phys.*, 2010, **81**, 174402.
80 M. Ziese, *J. Phys.: Condens. Matter*, 2001, **13**, 2919.
81 S. N. Kaul, *J. Magn. Magn. Mater.*, 1985, **53**, 5.
82 K. Huang, *Statistical Mechanics*, Wiley, New York, 2nd edn, 1987.
83 V. Franco, J. S. Blazquez and A. Conde, *Appl. Phys. Lett.*, 2006, **89**, 222512.
84 M. Pękała, *J. Appl. Phys.*, 2010, **108**, 113913.
85 V. Franco, J. S. Blázquez and A. Conde, *J. Appl. Phys.*, 2008, **103**, 07B316.
86 J. S. Amaral, N. J. O. Silva and V. S. Amaral, *J. Magn. Magn. Mater.*, 2010, **322**, 1569.